



## Design of cobalt gradient via controlling carbon content and WC grain size in liquid-phase-sintered WC–Co composite

Peng Fan<sup>a</sup>, Jun Guo<sup>a</sup>, Zhigang Zak Fang<sup>a,\*</sup>, Paul Prichard<sup>b</sup>

<sup>a</sup> Department of Metallurgical Engineering, University of Utah, 135 South 1460 East Room 412, Salt Lake City, UT 84112, USA

<sup>b</sup> Corporate Technology, Kennametal Inc., 1600 Technology Way, P.O. Box 231, Latrobe, PA 15650–0231, USA

### ARTICLE INFO

#### Article history:

Received 3 July 2008

Accepted 16 August 2008

#### Keywords:

Liquid phase sintering

Cemented carbide

Functionally graded materials

Liquid redistribution

Composition gradient

### ABSTRACT

WC–Co composites with a gradient of cobalt content can offer an improved performance as a cutting tool. During liquid phase sintering, a Co gradient can be created through Co redistribution induced by pre-designed gradients of WC grain size and/or C content in green parts. The driving force of Co redistribution is migration pressure, which is dependent of three factors – liquid Co volume fraction, WC grain size, and C content. In order to obtain a desired Co gradient, it is necessary to quantitatively understand the dependence of migration pressure as a function of the three factors. This study experimentally established the dependence of migration pressure as a function of C content and liquid Co volume fraction. Combining this result with the previously obtained dependence on WC grain size and liquid Co volume fraction enables the design of Co gradient via controlling carbon content and WC grain size.

© 2008 Elsevier Ltd. All rights reserved.

### 1. Introduction

Functionally graded cemented tungsten carbide (WC–Co) is a typical example of functionally graded materials with improved engineering performance due to the existence of a compositional gradient. For example, a WC–Co material with cobalt enriched surface offers an optimum combination of wear resistance and fracture toughness required for coated cutting tools. However, the manufacture of WC–Co with graded cobalt compositions via liquid phase sintering process is a difficult challenge, because the liquid cobalt phase tends to migrate from the locations with higher liquid Co volume fraction to the locations with lower liquid Co volume fraction during liquid phase sintering, which results in a homogeneous cobalt distribution within the material even if there was a Co gradient at the beginning of sintering [1–7]. A potential solution to this problem is to employ pressure-assisted solid-state sintering techniques such as HIPing or spark plasma sintering to consolidate the graded WC–Co compact at solid-state. However, these alternative processes have limited industrial applications because of two factors: first, the high-pressure processes are costly, and secondly the mechanical properties of materials produced by the pressure-assisted solid-state sintering process are often different from those produced by liquid phase sintering. Liquid phase sintering is the most viable option for manufacturing conventional as well as functionally graded WC–Co materials. The challenge is then to develop methods that either create or maintain a Co gradient during liquid

phase sintering. One of the methods is to introduce pre-designed gradients of WC grain size and/or C content in green compacts, since it has been found that WC grain size and C content affect the distribution of Co in liquid-phase-sintered WC–Co composites.

During liquid phase sintering, WC–Co system is a two-phase system consisting of solid WC grains immersed in liquid Co. Liquid Co redistribution or migration is an interfacial-energy-driven liquid flow phenomenon. This phenomenon is termed liquid phase migration whose driving force is termed migration pressure [1,8,9]. Anytime when the migration pressure is not homogeneous, liquid Co tends to migrate or redistribute so as to homogenize the migration pressure. For WC–Co with only pre-designed Co gradient, liquid phase migration will lead to the elimination of Co gradient. However, for WC–Co with pre-designed gradients of WC grain size and/or C content, liquid phase migration will either create or maintain a Co gradient, because the migration pressure is dependent of the three key factors – the volume fraction of liquid Co, WC grain size and C content. Consequently, the cobalt gradient in a WC–Co composite can be controlled by controlling the gradients of WC grain size and/or C content in green compacts. To do so, however, quantitative understandings of the dependence of migration pressure as a function of the above three key factors are required.

The dependence of migration pressure on WC grain size and liquid Co volume fraction has been reported previously [9]. In this study, the effect of carbon content on migration pressure was investigated. Co gradients in liquid-phase-sintered bi-layered WC–Co with each layer having different C contents in green compacts were examined. The dependence of migration pressure as a

\* Corresponding author. Tel.: +1 801 414 3251.

E-mail address: [zak.fang@utah.edu](mailto:zak.fang@utah.edu) (Z.Z. Fang).

function of the above three factors was quantitatively established in a single model, enabling the design of Co gradient via the control of carbon content and WC grain size. The result is expected to be valuable in design and manufacture of functionally graded WC–Co composite materials and components with improved performance.

## 2. Models of the dependence of liquid migration pressure on WC particle size, carbon content and liquid Co volume fraction

Lisovsky [1,10–12] experimentally studied the variation of liquid migration pressure,  $P_m$ , as a function of liquid volume fraction,  $u$ , for the WC–Co system. The liquid migration pressures of WC–Co samples with various Co contents was determined by measuring the radius of liquid Co surface filled in a V-shaped capillary, and the following empirical equation was obtained:

$$P_m = k_0[(1/u - 1)^{1/3} - 1.41u]/d \quad (1)$$

where  $P_m$  is the liquid migration pressure,  $k_0$  is a coefficient,  $u$  is liquid volume fraction, and  $d$  is solid particle diameter. According to Eq. (1),  $P_m$  is predicted to diminish when  $u = 0.61$ , which agrees with the experimental data of the variation of  $P_m$  with  $u$  for WC–Co system [11,12].

However, as pointed out by Suresh and Mortensen [14], the agreement of Eq. (1) with experiments including simultaneous variations in particle size and liquid volume fraction is poor. In a recent study by the present authors [9], it was also found that Eq. (1) has a poor agreement with experimental data with respect to the variation of  $P_m$  with WC particle size  $d$ . It was shown that the discrepancy between the experimental value and the predicted cobalt content could be as much as 100%. The discrepancy between Eq. (1) and experiments was attributed to the assumption of the linear relationship between  $P_m$  and  $1/d$ . This assumption may be valid in ideal composite systems in which mono-sized and isometric-shaped solid particles are uniformly distributed in a liquid phase matrix, while in real WC–Co composite materials there is a wide distribution in WC size, and WC particles are usually non-isometric in shape. The experimental study [9] established the dependence of liquid migration pressure on WC particle size and liquid Co volume fraction to be

$$P_m = k_1[(1/u - 1)^{1/3} - 1.41u]/d^{0.4} \quad (2)$$

where  $k_1$  is an empirical coefficient with the value of 2048.

It has been demonstrated that Eq. (2) is satisfactory when applied to WC–Co systems with stoichiometric carbon content. However, the equation has to be modified to include additional term to describe the effect of carbon content when WC–Co is not at stoichiometry. Therefore, the following equation is proposed in this study:

$$P_m = 2048(1 + b_1 \Delta x_{[C]} + b_2 \Delta x_{[C]}^2)[(1/u - 1)^{1/3} - 1.41u]/d^{0.4} \quad (3)$$

where  $\Delta x_{[C]}$  is the difference of molar fraction of C in liquid Co in respect to stoichiometry;  $b_1$  and  $b_2$  are empirical coefficients to be determined.

In order to determine exact values of  $b_1$  and  $b_2$ , consider a bi-layer configuration of a WC–Co specimen as shown in Fig. 1. The bi-layer is designed such that the C content in layer 1 is stoichiometric, i.e.,  $(\Delta x_{[C]})_1 = 0$ , while the C content in layer 2 is non-stoichiometric, i.e.,  $(\Delta x_{[C]})_2 \neq 0$ , but the WC particle sizes in the two layers are the same, i.e.,  $d_1 = d_2$ . Subscripts 1 and 2 denote layers 1 and 2, respectively. If the equilibrium liquid distribution is reached in the liquid-phase-sintered WC–Co bi-layer specimen, the liquid migration pressures in the two layers will equalize, i.e.,  $(P_m)_1 = (P_m)_2$ , which results in the following equation based on Eq. (3):

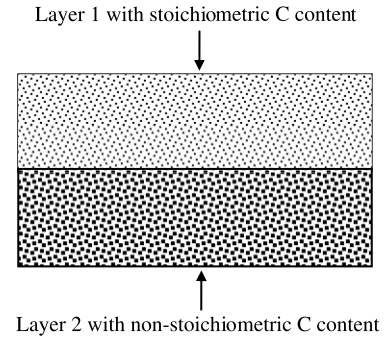


Fig. 1. Schematic of WC–Co bi-layer.

$$\frac{[(1/u_1 - 1)^{1/3} - 1.41u_1]}{[(1/u_2 - 1)^{1/3} - 1.41u_2]} = \frac{[1 + b_1(\Delta x_{[C]})_2 + b_2(\Delta x_{[C]})_2^2]}{[1 + b_1(\Delta x_{[C]})_1 + b_2(\Delta x_{[C]})_1^2]} \quad (4)$$

Rearranging this equation leads to

$$f = \frac{(1/u_1 - 1)^{1/3} - 1.41u_1}{(1/u_2 - 1)^{1/3} - 1.41u_2} = 1 + b_1(\Delta x_{[C]})_2 + b_2(\Delta x_{[C]})_2^2 \quad (5)$$

Using Eq. (5),  $b_1$  and  $b_2$  can be obtained by linear regression of experimental data of measured liquid Co volume fractions and C content in each of the two layers of a bi-layer WC–Co sample after equilibrium liquid distribution is reached. This equation serves as a theoretical model for us to investigate the dependence of  $P_m$  on  $\Delta x_{[C]}$ , by conducting liquid phase sintering experiments of bi-layer WC–Co materials.

## 3. Experimental

For the stoichiometric samples labeled as 6Co, 10Co and 16Co (where 6, 10 and 16 denote Co content, wt%), powders of WC and Co were mixed to prepare samples; for sub-stoichiometric ones labeled as 6CoA, 8CoA, 10CoA, etc., WC, Co and W were mixed; while for over-stoichiometric ones labeled as 6CoB, 8CoB, 10CoB, etc., WC, Co and graphite were used. Powders were mixed together with 2% paraffin wax, and then the powder mixture was milled in heptane in a Nalgene bottle containing WC balls for 14 h on a rolling mill. After milling, the powder mixture was dried in a rotary evaporator at 80 °C, and then compacted at 200 MPa into bi-layer disk-shaped samples, with each layer having different C and Co contents but the same WC particle size. The disk-shaped bi-layer samples were dewaxed at 300 °C before sintering.

Liquid phase sintering experiments were carried out in a vacuum furnace. WC–Co bi-layer samples were heated up at a rate of 10 °C/min to 1400 °C, held at that temperature for 5 min, and then quickly cooled down in the furnace by switching off the power. The liquid-phase-sintered bi-layer samples were polished and etched with Murakami's reagent. The Co contents across each layer of the bi-layer samples were measured using energy dispersive spectroscopy (EDS) incorporated with the scanning electron microscope (SEM), and then the average Co content in each layer was calculated. WC particle size,  $d$ , was represented by the mean linear intercept length measured on SEM photos of the sintered samples.

It is worth noting that the holding time of 5 min was sufficient for the Co redistribution to reach equilibrium based on previous studies [13] in which a bi-layer sample of the same geometry as in the present study was used. The two layers had stoichiometric carbon content and the same WC grain size; however, the two layers had different initial Co contents (6 and 16 wt% Co, respectively). After sintering by the exact same heating profile as used in the

**Table 1**  
Results of Co content, liquid Co volume fraction, WC particle size and difference of molar fraction of C in liquid Co phase in respect to stoichiometry

Layer 1					Layer 2				
Label	Co (wt%)	$u$	WC ( $\mu\text{m}$ )	$\Delta x_{\text{C}}$	Label	Co (wt%)	$u$	WC ( $\mu\text{m}$ )	$\Delta x_{\text{C}}$
10Co	9.43	0.2203	0.95	0	8CoB	8.67	0.1977	0.95	0.02484
10Co	8.44	0.1991	0.95	0	6CoB	7.56	0.1744	0.95	0.02484
10Co	11.26	0.2584	0.95	0	16CoA	14.05	0.3380	0.95	-0.01850
10Co	10.68	0.2465	0.95	0	14CoA	12.68	0.3087	0.95	-0.01850
10Co	9.96	0.2315	0.95	0	12CoA	11.51	0.2832	0.95	-0.01850
16Co	15.89	0.3491	0.95	0	14CoB	14.03	0.3030	0.95	0.02484
16Co	14.90	0.3304	0.95	0	12CoB	12.96	0.2828	0.95	0.02484
16Co	13.76	0.3084	0.95	0	10CoB	12.39	0.2719	0.95	0.02484
6Co	8.05	0.1906	0.95	0	12CoA	9.54	0.2390	0.95	-0.01850
6Co	7.24	0.1728	0.95	0	10CoA	8.43	0.2134	0.95	-0.01850
6Co	6.49	0.1561	0.95	0	8CoA	7.39	0.1889	0.95	-0.01850

present study, the initial Co gradient was found to be completely eliminated, indicating that Co redistribution due to liquid migration was a fast process and a 5 min holding at 1400 °C was sufficient for the Co redistribution to reach equilibrium.

Another issue concerning the dependence of cobalt migration on carbon content is that the difference in carbon content within the sample is expected to decrease with time. Based on the result of a separate study of the diffusion of carbon in WC–Co bi-layers [13], the rate of the change was found to be small within the short time period of liquid phase sintering in this study. This is qualitatively understandable because the diffusion path of carbon in the liquid cobalt is hindered by the presence of rigid WC skeleton. This difference in the kinetics of liquid cobalt migration and the carbon diffusion through the WC–Co composite makes it possible to control the cobalt distribution via the control of carbon gradient.

It was also found that the average WC grain size after sintering in each layer of the samples varied between 0.92 and 0.97  $\mu\text{m}$ . The measurement error is approximately 7%, suggesting that the effects of WC grain sizes were negligible under the condition of this study. An averaged value of 0.95  $\mu\text{m}$  was used to represent the WC grain size after sintering for all layers of all samples.

The composition of liquid Co, including molar fractions of C and W, was determined from the isothermal section of ternary Co–W–C phase diagram at 1400 °C [15]. The molar volume of liquid Co with different composition was calculated from the reported dependence of the molar volume of liquid Co as a function of the composition and temperature and the molar volume of WC [16]. Then liquid volume fractions of each layer of the bi-layer samples were calculated based on the Co content, the compositions of liquid Co and the molar volume of liquid Co.

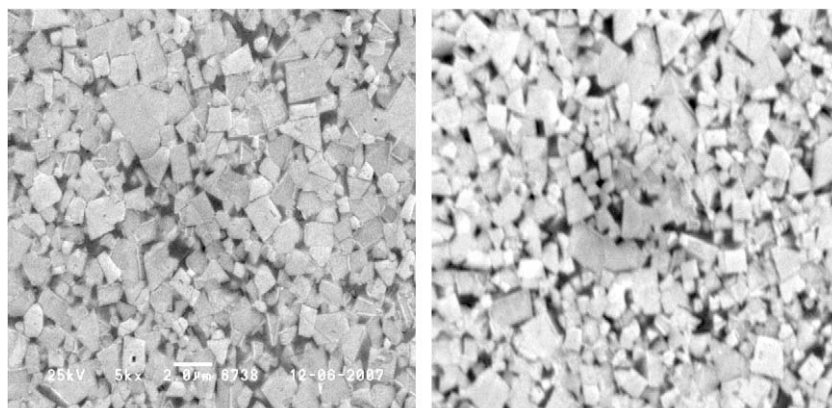
In Table 1, Co content, liquid Co volume fraction, WC particle size and molar fraction difference of C in respect to stoichiometry are listed, noting that all the above parameters were the values after sintering.

## 4. Results and discussions

### 4.1. Co content profile after sintering

Fig. 2 is the micrograph of a sintered sample, which shows that the samples had minimum porosity after sintering, consistent with the normal industrial practice. Co content after sintering was measured across the two layers of each bi-layered sample. It was found, as shown in Fig. 3, that Co content in the inner part of one layer was significantly different from that in the other layer, obviously demonstrating the effect of C content on migration pressure and Co distribution. It was also noted that the Co contents near the inter-layer boundary were usually higher than that at the inner part of each layer, while the Co contents near the two ends of the sample were usually lower. The former phenomenon may be attributed to some unclear effect of inter-layer boundary on Co distribution; while the latter may result from the carbonization of the sample surface during sintering, noting that higher C content induces lower Co content. In order to minimize these unclear effects, only the Co contents measured at inner locations of each layer, which were 1 mm away from the inter-layer boundary and 1 mm away from the two ends of the samples, were used to calculate the average Co content in each layer.

It is known that the shrinkage of WC–Co is dependent on C content [17,18], which may affect the final cobalt distribution. The



(a) in the layer of 10Co

(b) in the layer of 8CoB

**Fig. 2.** Micrographs of 10Co–8CoB sample after sintering, showing no porosity.

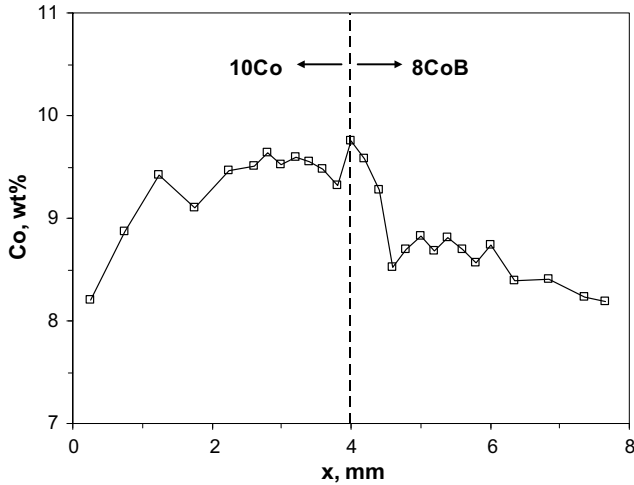


Fig. 3. Co content profile after sintering.

shrinkage of WC–Co can be divided into three stages. The first and the second stages occur below the melting point of the binder, which will not cause macroscopic migration of Co. Only in the third stage shrinkage may contribute, if any, to Co migration, since liquid Co starts to form in this stage. According to the experimental results by Peterson, for sub-stoichiometric, stoichiometric and super-stoichiometric compositions the third stage of shrinkage starts at 1370, 1360 or 1320 °C, respectively, and finishes within 1 or 2 min. Even if there is any significant Co migration due to the shrinkage (no evidence is available for this), the contribution from the shrinkage will stop before the temperature reaches the holding temperature of this study. Considering that the liquid migration is a fast process as mentioned in Section 3, the ‘memory’, if any, from shrinkage is expected to be negligible.

4.2. Dependence of  $P_m$  as a function of  $u$ ,  $d$  and  $\Delta x_{[C]}$

Using Eq. (5),  $b_1$  and  $b_2$  were obtained by linear regression based on the data of liquid Co volume fraction ( $u$ ) and molar fraction difference of C in liquid Co phase in respect to stoichiometry ( $\Delta x_{[C]}$ ) listed in Table 1. The obtained results were  $b_1 = -9$  and  $b_2 = 155$ .

The dependence of  $P_m$  as a function of  $u$ ,  $d$  and  $\Delta x_{[C]}$  is thus obtained as

$$P_m = 2048(1 - 9\Delta x_{[C]} + 155\Delta x_{[C]}^2)[(1/u - 1)^{1/3} - 1.41u]/d^{0.4} \quad (6)$$

where  $P_m$  is the liquid migration pressure, Pa;  $u$  is liquid Co volume fraction;  $\Delta x_{[C]}$  is the difference of molar fraction of C in liquid Co phase in respect to stoichiometry;  $d$  is WC particle size (linear intercept length), m.

The model can be considered as valid under the following conditions: (a) 1400 °C, (b) the compositions of WC–Co are such that there is neither eta phase nor graphite at the temperature and (c) WC grain size after sintering is from 0.95 to 7.5  $\mu\text{m}$ , based on the grain size domain studied for grain size effect [9].

For simplification, the model was established by assuming that there are no coupled terms of C content effect, WC grain size effect and liquid volume fraction effect. Therefore, the C content effect obtained in this study for a fixed WC grain size was assumed to be applicable to other grain sizes. The effect of WC grain size on cobalt migration as reported in a previous study [9] for stoichiometric compositions is expected to be applicable to non-stoichiometric compositions. Further studies will be needed to clarify whether the coupled term is needed to improve the current model.

4.3. Design of Co gradient by controlling C content and WC particle size

The establishment of the dependence of liquid migration pressure as a function of the volume fraction of the liquid Co phase, C content and the WC particle size is valuable for the design and manufacture of functionally graded WC–Co composite materials.

As mentioned in Section 2, the equilibrium liquid distribution is reached only when the liquid migration pressure is uniform throughout the composite material. For any given value of liquid migration pressure, the volume fraction of liquid Co phase varies with C content and WC particle size. A desired Co gradient can be acquired by pre-designing a suitable gradient of C content and WC particle size. This approach can be readily used to design various bi-layer, multi-layer, or continuously graded structures of WC–Co.

To illustrate the utility of Eq. (6), contour plots of  $P_m$  as a function of Co content and C content at a fixed WC particle size ( $=1 \mu\text{m}$ ) have been computed based on Eq. (6) and plotted in Fig. 4a. Any two points on the same contour line have the same liquid migration pressure and thus can represent the final or equilibrium Co and C contents in a bi-layer WC–Co structure. Therefore, these

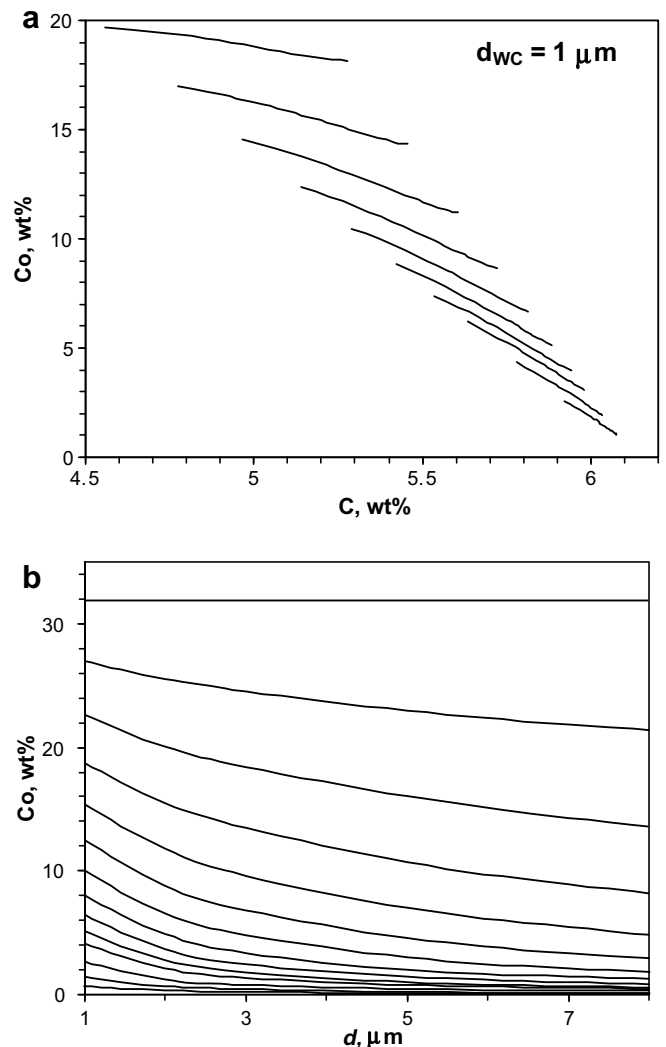


Fig. 4. Liquid migration pressure ( $P_m$ ) contour. (a) As a function of Co content and C content at a fixed WC particle size. (b) As a function of Co content and WC particle size at the stoichiometric C content. Each line represents one iso- $P_m$  line calculated from Eq. (6).

contour line plots can be used to design and fabricate WC–Co composite with Co gradient via controlling C gradient.

Similarly, contour plots of  $P_m$  as a function of C content and WC particle size at the stoichiometric C content have also been computed based on Eq. (6) and plotted in Fig. 4b. These contour line plots can be used to design and fabricate WC–Co composite with Co gradient via controlling WC particle size gradient.

It is possible to design and fabricate WC–Co with Co gradient via controlling both C content and WC particle sizes. For this purpose, contour surfaces (rather than contour lines) of  $P_m$  as a function of Co content, C content and WC particle size may be computed and plotted. However, contour surfaces are not as clearly informative as contour lines, so they are not constructed in this paper. A better way to do the design is to numerically solve Eq. (6). Suppose that a WC–Co bi-layer structure with the liquid Co volume fractions of  $u_1$  and  $u_2$ , respectively, needs to be fabricated via controlling both C content and WC particle size in each layer. According to  $(P_m)_1 = (P_m)_2$  and Eq. (6), it is necessary to have

$$[1 + b_1(\Delta x_{[C]})_1 + b_2(\Delta x_{[C]})_1^2][(1/u_1 - 1)^{1/3} - 1.41u_1]/d_1^{0.4} = [1 + b_1(\Delta x_{[C]})_2 + b_2(\Delta x_{[C]})_2^2][(1/u_2 - 1)^{1/3} - 1.41u_2]/d_2^{0.4} \quad (7)$$

Solving Eq. (7) with available values of  $u_1$ , and  $u_2$  can lead to a series of solutions of  $((\Delta x_{[C]})_1, d_1; (\Delta x_{[C]})_2, d_2)$ . Based on practical conditions, engineers can select one among the solutions to design the desired graded WC–Co.

From a manufacturing perspective, the temperature gradients within a production size vacuum furnace would require sintering hold time of much more than 5 min at 1400 °C in order to avoid metallurgical non-conformances. A longer hold time may cause the elimination of initial C gradient in the green parts due to C diffusion, especially for products of small sizes, thus eliminating the Co gradient. The dependence of the cobalt migration on time is the subject of a separate study.

## 5. Summary

During liquid phase sintering, a Co gradient can be created through Co redistribution induced by pre-designed gradients of WC grain size and/or C content in green parts. The driving force of Co redistribution is migration pressure, which depends on three primary factors – liquid Co volume fraction, WC grain size and C content. The present study experimentally established the dependence of migration pressure as a function of C content and liquid Co volume fraction. The result, in combination with the previously

reported study on the dependence cobalt migration on WC grain size and liquid Co volume fraction, enables the establishment of the dependence of  $P_m$  as a function of all three primary factors in a single model as follows:

$$P_m = 2048(1 - 9\Delta x_{[C]} + 155\Delta x_{[C]}^2)[(1/u - 1)^{1/3} - 1.41u]/d^{0.4} \quad (8)$$

where  $P_m$  is the liquid migration pressure, Pa;  $u$  is liquid Co volume fraction;  $\Delta x_{[C]}$  is the difference of molar fraction of C in liquid Co phase in respect to stoichiometry;  $d$  is WC particle size (linear intercept length), m. The equation can be applied to design and manufacture of WC–Co composite with Co gradient by controlling carbon content and WC grain size.

## References

- [1] Lisovsky AF. The migration of metal melts in sintered composite materials. *Int J Heat Mass Trans* 1990;33:1599–603.
- [2] Colin C, Durant L, Favrot N, Besson J, Barbier G, Delannay F. In: *Proceedings of 13th Plansee seminar*, vol. 2. 1993. p. 522.
- [3] Put S, Vleugels J, Van der Biest O. Functionally graded WC–Co materials produced by electrophoretic deposition. *Scripta Mater* 2001;45:1139–45.
- [4] Fang ZZ, Eso OO. Liquid phase sintering of functionally graded WC–Co composites. *Scripta Mater* 2005;52:785–91.
- [5] Fisher U, Waldenström M, Hartzell T. Cemented carbide body with increased wear resistance. US Patent 5,856,626; January 5, 1999.
- [6] Fischer UKR, Hartzell ET, Akerman JGH. Cemented carbide body used preferably for rock drilling and mineral cutting. US Patent 4,743,515; May 10, 1988.
- [7] Collin M, Norgren S. Hardness gradients in WC–Co created by local addition of  $Cr_3C_2$ . In: *Proceedings of the 16th international Plansee seminar*, Plansee, reutte, Austria, May, 2005.
- [8] Fan P, Fang ZZ, Sohn HY. Mathematical modeling of liquid phase migration in solid–liquid mixtures: application to the sintering of functionally graded WC–Co composites. *Acta Mater* 2007;55:3111–9.
- [9] Fan P, Eso O, Fang ZZ, Sohn HY. Effect of WC particle size on Co distribution in liquid-phase-sintered functionally graded WC–Co composite. *Int J Refract Metal Hard Mater* 2008;26:98–105.
- [10] Lisovsky AF. On the imbibition of metal melts by sintered carbides. *Powder Metall Int* 1987;19:18–21.
- [11] Lisovsky AF. Migration of metal melts in sintered composite bodies. Kiev: Naukova Dumka; 1984.
- [12] Lisovsky AF. Mass transfer of liquid phase in sintered composite materials when interacting with metal melts. *Int J Refract Metal Hard Mater* 1989;8:133–6.
- [13] Fan P, Guo J, Fang ZZ, Prichard P. unpublished work.
- [14] Suresh S, Mortensen A. *Fundamentals of functionally graded materials*. London: The Institute of Materials; 1998. p. 28.
- [15] Mahale AE. Phase diagrams for ceramists. *Am Ceram Soc* 1994;X.
- [16] Uhrenius B. Evaluation of molar volumes in the Co–W–C system and calculation of volume fractions of phases in cemented carbides. *Int J Refract Metal Hard Mater* 1993–1994;12:121–7.
- [17] Petterson A. Sintering shrinkage of WC–Co and WC–(Ti,W)C–Co materials with different carbon contents. *Int J Refract Metal Hard Mater* 2004;22:211–7.
- [18] Petterson A, Agren J. Sintering shrinkage of WC–Co materials with different compositions. *Int J Refract Metal Hard Mater* 2005;23:258–66.